Effects of high pressure and ohmic heating on shell loosening, thermal and structural properties of shrimp (Pandalus borealis)

Dang, Tem Thi; Feyissa, Aberham Hailu; Gringer, Nina; Jessen, Flemming; Olsen, Karsten ; Bøknæs, Niels; Orlien, Vibeke

Published in:
Innovative Food Science and Emerging Technologies

Link to article, DOI:
10.1016/j.ifset.2019.102246

Publication date:
2020

Document Version
Peer reviewed version

Effects of high pressure and ohmic heating on shell loosening, thermal and structural properties of shrimp (*Pandalus borealis)*

Tem Thi Dang[a], Aberham Hailu Feyissa[b], Nina Gringer[b], Flemming Jessen[b], Karsten Olsen[a], Niels Bøknæs[c], Vibeke Orlien[a,*]

[a] Department of Food Science, Faculty of Science, University of Copenhagen, Rolighedsvej 26, 1958 Frederiksberg C, Denmark

[b] National Food Institute, Technical University of Denmark, Søltofts Plads, Building 221, DK-2800 Kgs. Lyngby, Denmark

[c] Royal Greenland A/S, Hellebarden 7, DK-9230 Svenstrup J, Denmark

* Corresponding author at: Department of Food Science, Faculty of Science, University of Copenhagen, Rolighedsvej 26, DK-1958 Frederiksberg C, Denmark.

E-mail address: vor@food.ku.dk (V. Orlien).

Abstract

This study aimed at understanding the effects of high pressure (HP) and ohmic heating (OH) on the peelability, the underlying mechanisms of HP- and OH-induced shell tightening, the thermal and structural properties of shrimp parts. HP improved the peelability of shrimp at low pressure level (<350 MPa) and short holding time (≤3 min) and the optimum condition for peeling was at 100 MPa for 3 min at 5°C. However, a higher pressure level (>350 MPa) led to a decrease in the peelability. High pressure at 600 MPa stabilized cuticular and epidermal collagen and formed new collagen-like structures by new linkages, which strengthened the muscle-shell connection and reduced the peelability. Shrimp meat induced from HP at 100 MPa and 600 MPa had minorly denatured myofibrillar proteins. OH as a blanching method did not significantly improve the peelability of shrimp at most of the studied conditions. Some extreme conditions (e.g. at 50°C) caused a markedly low peelability due to occurrence of collagen gelatinization. The gel formation from collagen-gelatin transformation under heating added strength to adherence of shell to epidermis and muscle, as a consequence, a difficult peeling was experienced. OH also denatured proteins in shrimp meat and caused loss of astaxanthin.

Industrial relevance: The industrial processing of ready-to-eat shrimp involves the on-ice or in-brine maturation process which loosens the shrimp's shell from its meat, and therefore enable the mechanical peeling. However, the traditional maturation is time consuming (up to 4 - 5 days), inevitably leads to reduced quality of shrimp meat. This study shows the possibility of the application of HP at mild pressure levels to promote the shell loosening at short HP processing time (≤3 min). However, at more severe HP conditions could lead to the shell tightening which was caused by HP-induced stabilization of collagen in shell and epidermis. The study also shows that ohmic heating (<5 min) might not be a significant blanching method to support the maturation since OH had minor positive effect on shell loosening at

some OH conditions (e.g. 2 or 10% NaCl, 92V, and 30 or 35°C), but had a counter effect at most OH conditions especially at high temperature.

Keywords: shrimp; peeling; shell loosening; ohmic heating; high pressure; collagen

1. Introduction

Peeling is an important step in shrimp processing since the process can affect the yield, sensory, organoleptic and nutritional quality of final shrimp products (Dang et al., 2018a). The tight muscle-shell attachment causes difficulty in peeling freshly caught shrimp. Therefore, shell-loosening is needed to carry out as an essential pre-peeling step before the shrimp can be peeled in an automatic peeler. The most commonly used shell-loosening methods include empirical maturation of shrimp on ice and in brine for up to 4-5 days. However, as shrimp are highly perishable, such a long maturation could cause degradation in quality and risk of microbial growth in final products. A new method is therefore needed to both facilitate the peeling and meanwhile maintain the meat quality. In order to address the issue, our earlier studies (Dang et al., 2018b, 2018c) attempted to apply enzymes and/or ultrasound on shrimp peeling and quality, and found some positive results. Being inclined to green and novel application, more explorations have been continued to other emerging technologies, i.e. high pressure and ohmic heating.

High pressure has increasingly gained interests among food researchers mainly due to its ability to improve food quality and safety (Dang et al., 2018a). Although some attempts have been made to apply high pressure in facilitating deshelling shellfish, e.g. oysters, clams, and mussels, (Bindu, Grinson, Kamalakanth, & Gopal, 2015; He, Adams, Farkas, & Morrissey, 2002; Hsu, Hwang, Chi, & Lai, 2010; Voisin, 2001), less attention has been paid on shrimp peeling. Scarcely, in an American Society of Agricultural and Biological Engineers meeting paper by Yang et al. (2010), HP was tested on peelability, tail integrity, drip loss and color changes of white shrimp (*Penaeus vannamei* Boone*)*. It was found that HP at 200 MPa for three minutes improved those tested attributes. Particularly, HP-treated shrimp had the tail being less lost during peeling, drip loss being reduced by half, color remaining unchanged, all compared to untreated shrimp. Pressure appeared to promote water movement into the shrimp and to denature protein that enhanced water holding capacity due to exposure of water binding sites at the

protein surface. However, HP-induced changes in thermal-stable and structural properties of shrimp have not been investigated by far.

Ohmic heating is a thermal method which involves dissipation of electrical energy to heat, due to the electrical resistance of the food (Jaeger et al., 2016). Ohmic heating is used to precook, blanch, cook and sterilize vegetables, fruit, and meat (Allali, Marchal, & Vorobiev, 2010; Mesias, Wagner, George, & Morales, 2016; Sengun, Turp, Icier, Kendirci, & Kor, 2014; Zell, Lyng, Cronin, & Morgan, 2010). Ohmic heating is found to be efficient in tomato peeling (Wongsa-Ngasri & Sastry, 2015, 2016a, 2016b). The use of ohmic heating was addressed to a reasonably short time over traditional steaming, an improved diffusion of peeling media through tomato skin, an improved firmness of peeled tomato, and reduction of peeling agent (lye). However, based on our current knowledge, no previous studies have been conducted on shrimp peeling. The potential of ohmic heating on shrimp peeling was assumed and recommended for future investigation in a previous study on effect of ohmic heating on shrimp quality (Pedersen, Feyissa, Kavli, & Frosch, 2016). In comparison with conventional steam, ohmic heating was found to be more uniform and faster in cooking different parts of shrimp (head, body, and tail), comparable texture and drip loss, and less color difference (Lascorz, ToreIla, Lyng, & Arroyo, 2016; Pedersen et al., 2016).

Proteins are the major components in shell and meat part of shrimp (Heu, Kim, & Shahidi, 2003; Rodde, Einbu, & Varum, 2008). Proteins are the main contributors to the textural and functional properties (e.g. texture, solubility, extractability, viscosity and water holding capacity), which are associated with the quality of shrimp (Herrero, 2008). Therefore, information on protein structure will provide a precise assessment on the textural and functional properties of shrimp. Spectroscopic methods have been used to obtain structural changes occurring during food processing (Herrero, 2008). Fluorescence spectroscopy is, for instance, a rapid and nondestructive technique exhibiting a huge

potential in food quality assessment based on descriptive and predictive methods (Karoui & Blecker, 2011). In principle, a fluorescent molecule (fluorophore) absorbs energy of UV/VIS light at a specific wavelength and emits it at higher wavelength (Hassoun & Karoui, 2017). A excitation-emission matrix (EEM) forms a fluorescence landscape allowing to obtain more information about fluorophores present in the sample (Hassoun & Karoui, 2017). EEM fluorescence spectroscopy has been used to monitor the freshness of fish over a storage period by tracking changes in fluorescence intensity of certain intrinsic fluorophores (aromatic amino acids, lipids and pigments) of fish (Dufour, Frencia, & Kane, 2003; ElMasry et al., 2015; ElMasry, Nakazawa, Okazaki, & Nakauchi, 2016). Changes of fluorescence behavior during treatment (e.g. high pressure, heating) also allowed assessment of toughness of quality attributes such as palatability of beef meat (Swatland, Nielsen, & Andersen, 1995), and tenderness of beef meat (Egelandsdal, Wold, Sponnich, Neegård, & Hildrum, 2002). Fluorescence studies on meat and seafood reported in the literature are dominated by fluorophore of collagen, tryptophan, NADH, vitamin A, and fluorescent oxidation products (Hassoun & Karoui, 2017; Karoui & Blecker, 2011). Therefore, identifying changes of fluorophore behavior of shrimp during treatments (e.g. high pressure, ohmic heating, steaming, enzyme hydrolysis) may help assess the effect of the treatments on shrimp quality. In addition to fluorescence spectroscopy, Raman spectroscopy is also very useful for studying structural changes that occur during treatment (Herrero, 2008). By monitoring changes in spectral bands, one can obtain information about α-helix, β-sheet structures of protein, consequently predict the quality of food (Herrero, 2008). Raman spectra also give useful information on other biocomponents such as lipids, pigments, polysaccharides, water, calcites etc. (LiChan, 1996).

The objective of this work was to study the effect of high-pressure treatment and ohmic heating on the peelability, the thermal and structural properties of body parts (shell and meat) of cold water shrimp, and to understand the mechanisms associated with peeling.

2. Materials and methods

2.1. Materials

Cold water shrimp (*P. borealis*) were provided by Royal Greenland A/S (Svenstrup, Aalborg, Denmark). The shrimp (160 – 200 shrimp/kg in size) were individually frozen, packed in carton packages and stored at −21°C. Fine table salt (NaCl) was obtained from a local supermarket (Copenhagen, Denmark). Endocut 03L (Endo3) and Tail21 enzyme preparations were obtained from Tailorzyme A/S (Sørborg, Denmark) and stored at 4 – 5°C until use. Endo3 is a food-grade endoprotease with broad specificity (60 Units/g) produced from *Bacillus clausii* whereas Tail21 is also a food-grade endoprotease but with high specificity (65 Units/mL) produced from fungi *Rhizomucor miehei*, as stated by the manufacturer.

2.2. High pressure

Frozen shrimp were thawed in tap water (~12°C) for 20 minutes. Thawed shrimp were packed in a Nalgene HDPE plastic bottle and the bottle was fully filled with chilled distilled water (5°C) and sealed with a cap. The bottle was placed in a pressure vessel submerged in hydrostatic fluid medium and pressurized in a Food Processing high pressure unit (QFP-6, Avure Technoliges AB, Vesterås, Sweden) between 100 – 600 MPa for 30 s – 3 min at 5 – 20°C. These selected ranges of parameters were based on the preliminary experiments in which peelability (by hand) and quality (texture and color by observation) of shrimp pressurized at extended ranges were considered. Immediately after high pressure treatment, shrimp were placed in ice water bath.

Response surface methodology (RSM) based central composite design (CCD) was chosen to evaluate the effect of three processing conditions i.e. pressure (P, 100 – 600 MPa), time (t, 0.5 – 3 min), and temperature (T, 5 – 20°C) on peeling work. The complete design consisted of 18-treatment

129 combinations including four replicates at central point. Two replicates were conducted for 14 treatments
130 at factorial points. Each treatment was performed on ten shrimp. Data analysis was performed using the
131 software SAS 9.4 (SAS ® Institute Inc., Cary, New York). Experimental data were fitted to a second-
132 order polynomial model Eq. (1) and regression coefficients were obtained.

$$Y = \beta_0 + \sum_{i=1}^{3} \beta_i X_i + \sum_{i=1}^{3} \beta_{ii} X_i^2 + \sum_{i=1}^{2} \sum_{j=i+1}^{3} \beta_{ij} X_i X_j \quad (1)$$

133 Where Y represents the response variable (peeling work, mJ/g), β_0 is intercept, β_i, β_{ii}, and β_{ij} are
134 coefficients of the linear, quadratic and interaction effect, respectively. X_i and X_j are the independent
135 variables (P, T, t).

136 **2.3. Ohmic heating**

137 A laboratory scale ohmic heater (BCH Ltd., Landcashire, UK) used to blanch shrimp consisted of
138 a voltage regulator (0 – 230 V, 60 Hz, 40 A) suppling power to a rectangular polyethylene heating cell
139 through two titanium electrodes positioned at two ends of the cell. The cell had inner width of 9.5 cm
140 and inner length of 12 cm (also distance between the electrodes). Voltage and electric current were
141 recorded by a built-in data logger system, and temperatures were monitored using a K-type thermocouple
142 connected with TC-08 data logger (Pico Technology, Cambridgeshire, UK).

143 Frozen shrimp (~120 g) were thawed in tap water bath for 20 min and then were placed into the
144 heating cell. NaCl solution (400 mL, 2% or 10% w/v concentration) was prepared and added to ohmic
145 heating cell and then the shrimp were placed within solution and heated to the desired temperature. The
146 shrimp were heated to different temperature (30, 35, 40, 50 and 60°C) and at different voltages (92, 138
147 and 184 V). Immediately after treatment, the shrimp were cooled in an ice water bath for 1 min before
148 maturing in 2% NaCl for 24 h at 2°C. The matured shrimp were washed with ice water and then placed
149 under ice cubes during peeling.

2.4. Peelability

The shrimp peelability was measured using the method reported in our earlier study (Gringer et al., 2018). In the present study, peeling work will represent the peelability of shrimp. Briefly, the three first abdominal segments of shrimp without legs were cut off, weighed (m_i) and horizontally hold by a pin attached to a customized fixture. The edge of the C-shaped shell of the three-segment portion was clamped by a clip attached to the texture analyzer (TA, 1000-g cell load, Brookfield AMETEK Inc., Middleboro, Massachusetts, USA) as the probe. The tension test was implemented to vertically pull off the shell from the meat (the peeling process). After the peeling, the shrimp was classified as completely peeled or incompletely peeled, and peeling work was calculated. The completely peeled shrimp was the shrimp having no shells remaining on the meat. The incompletely peeled shrimp having any shells remaining on the meat. The peeling work (mJ/g shrimp) was defined as the work required to pull off the shell from the three abdominal segments. The lower peeling work corresponded to the easier peeling. The peeling work calculation was based on the force-distance curve by multiplying the force by the distance of shell pulling and dividing by the weight of the three segments (Eq.(2)). Only the peeling work obtained from the completely peeled shrimp are presented and evaluated.

$$W = \frac{Fd}{m_i} \tag{2}$$

Where: W (mJ/g) is the work. F (N) is force applied to peeling. d (mm) is distance pulling the shell off. m_i (g) is initial weight of three segments with shell before peeling.

2.5. Differential scanning colorimetry (DSC)

Two HP treatments: 100 MPa for 1.75 min at 12.5°C (HP100) and 600 MPa for 1.75 min at 12.5°C (HP600) and two OH treatments: 10% NaCl, 138 V, and 30°C (OH30) and 10% NaCl, 138 V, and 50°C (OH50) were selected to evaluate the thermal and structural properties. HP100 and OH30 represented

171 rather good peeling treatments in high pressure and ohmic heating, respectively, whereas HP600 and
172 OH50 represented rather bad peeling treatments in high pressure and ohmic heating, respectively.

173 DSC measurements were carried out with Mettler Toledo DSC I calorimeter, which is based on the
174 heat flux principle. Calibration of heat flow and temperature was done with indium (T_m = 156.6°C, ΔH_{fus}
175 = 28.5 J/g) and zinc (T_m = 419.5°C, ΔH_{fus} = 107.5 J/g) as standards. A sample of ~10 mg was placed in
176 Mettler Toledo 40-µL standard aluminum crucible with pin and sealed with a lid. Measurements were
177 made at 10°C/min scan rate in the temperature range 20-80°C. Two to four replicates per treatment were
178 performed depending the availability of sample, and the results were presented as the average of the
179 replicates. DSC thermogram analysis was carried out using STARe software (Mettler Toledo).

180 **2.6. Spectroscopy**

181 For better understanding of structural behaviors of shrimp parts (shell and meat) subjected to two
182 main technologies: HP and OH, several other shrimp subjected to other techniques such as steam,
183 Endocut 03L protease (Endo3), Tail21 protease (Tail21), and sodium chloride were added to
184 spectroscopic measurements. Steam is a traditional thermal process and thus was selected to monitor the
185 thermal effect in HP (if any) and OH. Shrimp were steamed for 90 s (shrimp temperature 90°C). Endo3
186 and Tail21 have been the most and least, respectively, effective enzymes in shrimp shell-loosening in
187 our earlier study (Dang et al., 2018b), and were selected to evaluate the shell-loosening aspect and
188 structural changes associated with shell-loosening. Shrimp were submerged in an enzyme solution (2%
189 NaCl, 0.5% enzyme, and water) for 20 h at 5°C with continuous agitation. Sodium chloride (NaCl) was
190 selected to evaluate ionic effect as well as mimic a commonly used maturation method in shrimp industry.
191 Shrimp were submerged in 2% NaCl solution for 24 h at 5°C with continuous agitation.

2.6.1. Fluorescence spectroscopy

Fluorescence spectroscopic measurements were taken from the surface of shrimp parts (shell and meat) using a Cary Eclipse fluorescence spectrophotometer (Varian Inc., Palo Alto, California, US) through a double arm optical fiber probe bundle (C Technologies, Cedar Knolls, NJ). The probe was set at 45-degree angle and the sample end of the probe was kept at 5-mm distance from the sample. Excitation spectra were recorded in the 270-380 nm range with a 10-nm interval, and emission spectra were recorded in the 270 – 520 nm range with a 2-nm interval. The excitation and emission ranges were chosen based on preliminary survey scans. Both slit widths were set to 5 nm, and the scanning speed was 12,000 nm/min. Intensity data were plotted in an excitation emission matrix (EEM). Four to seven measurements were performed on two to four shrimp for each treatment.

2.6.2. Raman spectroscopy

A Bruker RAM II Raman Spectrometer (Karlsruhe, Germany) was used to obtain the Raman spectra, which were acquired and processed with the Opus software (Bruker, Karlsruhe, Germany). Ground freeze-dried sample was placed on a stainless steel cup, and then laser light with power of 400 mW was focused on the solid sample. Each spectrum was collected at room temperature under the following condition: 8 cm^{-1} resolution, 5-min scan time (~365 scans), over 3500 – 100 cm^{-1}. The Raman spectra of each sample were obtained in triplicate and the results were recorded as the average of the triplicate.

2.7. Data analysis

One way and multiway ANOVAs and RSM analysis were performed using SAS statistical software (version 9.4, SAS ® Institute Inc., Cary, NY). Mean comparison among treatments was performed by Student-Newman-Keuls test.

3. Results and discussion

3.1. High pressure on peelability

Pressure level is an essential parameter in any HP experiments. Its individual effect on shrimp peeling work when time and temperature are fixed at 1.75 min and 12.5°C is presented in **Figure 1A**. As seen, low pressure level (<350 MPa) offered a lower peeling work than that of control shrimp. However, its interactions with time and temperature in a HP system are of importance to optimize a processing condition.

The peeling work of shrimp pressurized at various conditions was measured. The RSM results obtained from various high pressure treatments were fitted to Eq. (1) and a complete second-order polynomial regression model Eq. (3) was obtained. The ANOVA and lack of fit test showed that the total model was significant (p <0.05) for fitting the response, and adequately represented the real relationship between tested parameters and response ($p_{\text{lack-of-fit}}$ >0.05). The determination coefficient (R^2) of the model was 0.51, which referred 51% of variations that could be explained by the fitted model (**Figure 1B)**. The linear and interaction effects were more significant than quadratic effects. Interaction between pressure and time was the most significant term (p = 0.047) in the model. Amongst the three factors studied, pressure had the most significant overall effect (p = 0.019) (i.e. sum of linear, quadratic, pressure-time interaction and pressure-temperature interaction effects of pressure factor), followed by pressurization time (p = 0.052) (i.e. sum of linear, quadratic, time-pressure interaction and time-temperature interaction effects of time factor), and finally least important temperature (p = 0.676) (i.e. sum of linear, quadratic, temperature-pressure interaction and temperature-time interaction effects of temperature factor).

$$W = 11.11 - 0.011P - 0.895t - 0.06T + 0.004Pt + 7.6 * 10^{-5}PT + 0.088Tt + 9 * 10^{-6}P^2 - (\quad (3)$$
$$T^2$$

235 Where: P is pressure (MPa), t is time (min), and T is temperature (°C).

236 The contour response surface plots varying two independent factors when the third factor kept
237 constant at its middle level are shown in **Figure 1C-D**. Increasing pressure or time resulted in increases
238 in the peeling work, whereas temperature appeared to have less significant effect on peeling work. The
239 peeling work decreased with decreases of pressure and time, reaching lowest peeling work (two lines 8
240 in contour plot **Figure 1C**) at either a pressure of 100 – 200 MPa and time 2.5 – 3 min or 250 – 600 MPa
241 and 0.5 min at fixed temperature of 12.5°C. When pressurization for 1.75 min at any temperature (5 –
242 20°C), pressures from 100 – 350 MPa had similar effect to one another on peeling work, but increasing
243 pressure at range 350 – 600 MPa resulted in increases in peeling work (**Figure 1D**).

244 The calculation of lowest predicted peeling work was performed based on Eq. (3) in order to
245 establish the optimum HP condition for peeling. The criteria for calculation included pressure range from
246 100 to 600 MPa with 10-MPa interval, time range from 0.5 to 3 min with 0.1-min interval, and
247 temperature range from 5 to 20°C with an interval of 1°C. The result showed that the optimum condition
248 to obtain the lowest peeling work (6.6 mJ/g) was positioned at 100 MPa, 3 min and 5°C. This peeling
249 work was 2.1 mJ/g lower than that of the control shrimp. However, the optimum condition was not
250 validated by experiment, since it is out of scope of this study.

251 **3.2. Ohmic heating on peelability**

252 Effect of ohmic-heating blanching (OH blanching) on shrimp peeling work is shown in **Table 1**.
253 Generally, OH blanching at most of studied conditions did not improve the peelability of subsequent salt
254 matured shrimp. Comparing means of all samples showed that all OH-treated shrimp had similar or
255 significantly higher peeling work than control shrimp (unblanched and matured in 2% NaCl for 24 h).

Three-way ANOVA showed that all the three OH parameters, i.e. salt concentration, voltage and temperature significantly influenced the peeling work. Interactions between salt and voltage and between salt and temperature were significant whereas interaction between voltage and temperature was not significant. Increasing voltage and temperature resulted in increases in the peeling working, probably due to transition of collagen into gelatin that was able to strengthen muscle-shell connection or fill existing shell-loosening gap (details described in section below).

3.3. Shell and meat characteristics

3.3.1. Thermal properties by differential scanning calorimetry (DSC)

DSC analysis was performed to understand thermal properties of shrimp parts after high pressure and ohmic heating treatments. **Figure 2** shows the DSC thermograms of parts of shrimp after high pressure and ohmic heating treatments. For epidermis, the endothermic peak at ~55°C was seen in raw, HP100, HP600 and OH30 samples but disappeared in OH50. Two additional peaks at ~58°C and 69°C were seen in HP100 epidermis, and a small peak at ~65°C newly appeared in OH30. No peaks were observed in the OH50 thermogram, indicating that OH50 denatured all proteins in epidermis. The transition peak at 55°C was identified as sarcoplasmic and connective (collagen) proteins based on previous studies in shrimp (Schubring, 2009; Sriket, Benjakul, Visessanguan, & Kijroongrojana, 2007; Verhaeghe et al., 2016). The 55°C peak in raw epidermis shifted towards 56°C in OH30 epidermis and 57°C in HP600. Additionally, enthalpy of transition increased from 0.07 J/g in raw epidermis to 0.19 J/g in OH30 and to 0.63 J/g in HP600 epidermis. The change in the endothermic peak temperature and the increased transition enthalpy suggest that OH30 and HP600 stabilized the structure of sarcoplasmic and connective proteins at different extent (Potekhin, Senin, Abdurakhmanov, & Tiktopulo, 2009). The existence of new peaks in the thermogram after high pressure treatment was also previously observed in pressurized fish muscle, which were attributed to the formation of structures that were stabilized by

hydrogen bonds (Angsupanich, Edde, & Ledward, 1999; Angsupanich & Ledward, 1998; Schubring, 2005). When pressure level increased from 100 MPa to 600 MPa, the two peaks of sarcoplasmic/connective proteins merged to become a broader peak. This indicates that increasing pressure, at least to 600 MPa, led to an accelerated formation of new structures that were similar to native sarcoplasmic/connective proteins and an increased stabilization of native sarcoplasmic/connective proteins.

For shell, DSC thermograms displayed one large endothermic peak at 44 – 45°C in raw and all treated shells. The peak was assigned to the helix-coil transition temperature of collagen as the most abundant protein (60-75%) in total proteins of shrimp shell (Ong, Danujatmiko, Aylianawati, & Sudaryanto, 2014) and also the major structural protein found in skin and bone of all animals (Wasswa, Tang, & Gu, 2007). The transition temperature slightly decreased with increasing high pressure by a maximum of 0.8°C at the highest pressure level (600 MPa) compared to raw shell. However, the enthalpy change (ΔH) and half-width temperature increased with increasing pressure, indicating pressure-induced stabilization of collagen structure. This pressure-induced stabilization was observed in pig acid-soluble collagen (Chen, Ma, Zhou, Liu, & Zhang, 2014; Potekhin et al., 2009) and bullfrog skin collagen (Nan et al., 2018). Some interpretations could be addressed to this phenomenon. Chen et al. (2014) suggested that high pressure at 500 MPa was speculated to form new hydrogen bonds between collagen and water and promoted the aggregation of collagen. Nan et al. (2018) attributed the stabilization to the dominance of axial pressure (pressure perpendicular to collagen axis) which compressed and strengthened the triple-helix structure of collagen. The thermal stability of collagen could also be related to the state of intermolecular crosslinks that are of importance in stabilization and continuity of molecules of collagen (Kopp, Bonnet, & Renou, 1990). Accordingly, high pressure might introduce new crosslinks or promote stronger existing crosslinks, in effect stabilizing the collagen structure.

302 In contrast to HP-treated shells, both transition temperature and ΔH were lower in OH-treated shells
303 than in the raw shell. This indicates that OH readily denatured cuticular collagen even at low temperature
304 30°C to lesser extent and accelerating extent at 50°C. Due to a short holding time (~10 s) at 50°C in OH,
305 the OH-induced denaturation of collagen was partial. Partial denaturation of collagen by OH could be
306 the reason of increasing peeling work (**Table 1**) that challenged the shrimp peeling. When collagen is
307 heated, intramolecular hydrogen bond breakage results in shrinkage of the collagen fibers, followed by
308 solubilization and gelatinization (Kopp et al., 1990). The collagen gelatinization formed a gel that was
309 able to glue the shell to the epidermis and the meat, consequently separation of the shell from meat was
310 difficult.

311 For muscle, a visible peak at ~39°C was present in raw muscle and other treated muscles, except
312 for muscle treated with OH50. This peak was assigned to the denaturation temperature of myosin
313 (Schubring, 2009). This temperature was higher than the 37.1°C reported by Schubring (2009) for the
314 same shrimp species. The myosin peak slightly decreased with increasing pressure both in enthalpy and
315 temperature values, indicating partial denaturation caused by high pressure. High pressure was also found
316 to denature myosin of ocean perch, saithe, herring fish muscle (Schubring, 2005). Like high pressure,
317 OH30 destabilized the structure of myosin, evidenced by decline in both enthalpy and temperature values
318 of the myosin peak. OH50 completely denatured myosin and the peak disappeared. This finding is in
319 agreement with the result from Schubring (2009) that the peak disappeared after preheating the shrimp
320 muscle at 45°C. The DSC equipment used was not able to detect actin peak, yet actin was found to be
321 more resistant to heat than myosin (Schubring, 2005).

322 **3.3.2. Raman spectra of shrimp**

323 The main composition of shrimp meat (*P. borealis*) comprises of protein (84%, dry matter basis),
324 lipid (2.5%, dry matter basis), ash (10%, dry matter basis) (Heu et al., 2003). The shell contains 33 –

325 40% protein (dry matter basis), 17 – 20% chitin (dry matter basis), and 34% ash (mainly calcium
326 carbonate, dry matter basis) (Rødde, Einbu, & Vårum, 2008). Chitin is a modified polysaccharide that
327 contains nitrogen in their polymerized N-acetylglucosamine structure (Raabe et al., 2006). Vibrational
328 spectra of chitin and protein share many common peaks, especially amide groups. Characterization of
329 the distinct peaks of chitin has previously been attempted by purification and fractionation (Hejazi,
330 Behzad, Heidarian, & Nasri-Nasrabadi, 2018; Rahman & Halfar, 2014), but the results were not in
331 agreement. Hejazi et al. (2018) reported that the peak at ~1540 cm^{-1} was one of indicative peaks for a
332 complete protein removal, whereas Rahman and Halfar (2014) reported that peaks distinguished from
333 the presence of collagen position in the fingerprint polysaccharide regions <900 cm^{-1}. The inconsistence
334 in the findings can arise from the difficulty of complete separation of chitin from collagen in a
335 mineralized chitin-collagen matrix (Raabe et al., 2006). Under taxonomic point of view, lobster and
336 shrimp belong to the crustacean group, therefore discussion concerning a mineralized chitin-collagen
337 matrix of shrimp will refer to a mineralized chitin-collagen matrix of lobster reported by Raabe et al.
338 (2006). In this context, the chitin nanofibril is coated by collagen fibrils, thus it is assumed that collagen
339 will be more susceptible to treatments and that collagen will be addressed in discussion when analyzing
340 spectra of shrimp shells.

341 FT-Raman spectra of shrimp meat and shell subjected to high pressure, ohmic heating, steam,
342 enzyme, and salt are presented in **Figure 3**. In general, structures of elements in meat were less
343 susceptible to the treatments than structures in shell. As for meat, the band from 1625 to 1700 cm^{-1} was
344 assigned to amide I, which is mainly due to C=O stretching and minor contribution from N-H in-plane
345 bending (LiChan, 1996). The amide I band is useful for the investigation of secondary structure (LiChan,
346 1996). The amide I peak was positioned at 1658 cm^{-1} for raw meat and all treatments except for OH50
347 and steam. The peak shifted toward 1665cm^{-1} and became slightly broadened in OH50 and steam meat.

348 The shifting and broadening during heating were indicators of the gradual loss of α-helix structure and
349 increased formation of β-sheet and random coil (David, Foley, Mavon, & Enescu, 2008; Ngarize,
350 Herman, Adams, & Howell, 2004), which was associated with heat denaturation. Thus, OH50 and steam
351 denatured the meat proteins to some extent. OH50-treated meat reduced the peak intensity at 1518 cm^{-1},
352 which, together with the peaks at 1156 and 1006 cm^{-1}, are characteristics of carotenoids (mostly
353 astaxanthin in shrimp) (Rau et al., 2017). This finding suggests that loss of some astaxanthin pigments
354 in shrimp meat could occur either during ohmic heating at 50°C or during peeling. It is noteworthy that
355 OH50-treated shrimp had a higher peeling work compared to the non-OH treated control shrimp (9.8
356 mJ/g vs 4.2 mJ/g, respectively) and being difficult to peel, thus attempts to pull the shell off probably
357 removed some surface pigments on shrimp meat. Interestingly, the overall spectrum of Endo3-treated
358 meat was similar to that of raw meat, suggesting that the most shell-loosening effective enzyme did not
359 affect the meat quality of shrimp.

360 As seen from **Figure 3**, more peaks in the Raman spectra of the shell were affected by the
361 treatments. Heat denaturation of protein (mainly collagen) happened to steam and OH50 shells,
362 evidenced by the shifting and broadening of the amide I peak (1658 cm^{-1}). The characteristic peaks of
363 carotenoids (1518, 1158, and 1004 cm^{-1}) in shells treated with OH50 and Tail21 increased in intensity
364 compared to other samples, indicating an increase of carotenoids in OH50- and Tail21-treated shell. The
365 increased pigments in OH50 shell were likely transferred from the meat. As mentioned above, OH50-
366 treated meat lost a certain amount of carotenoids. The pigment transfer was indeed due to the difficult
367 peeling of OH50-treated shrimp. The attempts to pull off the shell from the meat of an insufficiently
368 shell-loosened shrimp resulted in the pulling off some meat that were attached tightly to the shell.
369 Pigments adhered in the pulled meat were therefore lost in the remaining meat (Raman spectra obtained)
370 but appeared in the shell (Raman spectra obtained). The increased pigments in Tail21 shell were

371 enzymatically liberated from protein-pigment binding. The peaks at 1374 and 1079 cm^{-1} disappeared in
372 OH50 shell, indicating $CaCO_3$ decreased by ohmic heating 50°C (Chen, Yang, Zhong, & Yan, 2017).
373 The peak at 760 cm^{-1} was found to be diminished in samples containing NaCl in their maturation solution,
374 i.e. NaCl, Endo3 and Tail21, and this peak was assigned to tryptophan (Nonaka, Lichan, & Nakai, 1993).
375 The peak 1448 cm^{-1} contributed by CH_2-CH_3 bending in protein (Alimova et al., 2009) was slightly more
376 intense in OH50 and HP600 samples. This peak was insensitive to changes in protein secondary structure
377 but sensitive to the concentrations of CH_2 and CH_3 groups. The change of this peak was likely caused by
378 the formation of new components in the biological system (Alimova et al., 2009).

379 **3.3.3. Fluorescence spectra of shrimp**

380 The excitation-emission fluorescence landscapes of shrimp meat and shell are presented in **Figure**
381 **4**. Three dominant peaks 300/350 nm ($\lambda_{Ex\ max}/\lambda_{Em\ max}$), 330/410 nm and 330/490 nm were present in both
382 meat and shell and were assigned to tryptophan (the first peak) and collagen (the second and third peaks)
383 (Andersen & Wold, 2003; ElMasry et al., 2016). The signal of tryptophan was stronger in raw meat than
384 raw shell, whereas the signal of collagen was weaker in raw meat than in raw shell. This result suggests
385 that shrimp meat consisted of more tryptophan and less collagen than shell does. The signal of tryptophan
386 became stronger when meat were treated with high pressure 100 and 600 MPa, ohmic heating 50°C,
387 steam, enzymes Endo3 and Tail21, and NaCl, and when shell treated with all studied treatments. In meat,
388 tryptophan fluorescence appeared to be highly dependent on temperature and pressure since the intensity
389 was markedly high in high-level pressure and high-level temperature samples (i.e. HP600, OH50, and
390 steam). Moreover, the maximum emission of tryptophan fluorescence shifted from 340 nm in native meat
391 to 346 nm in the meat treated with the three treatments. This shifting (also known as red shift) indicates
392 that the exposure degree of tryptophan residues to the surrounding environment increased and the
393 conformation of protein changed (Vivian & Callis, 2001). Tryptophan residue is essentially buried in the

interior of the protein by other residues (also called quencher) (Vivian & Callis, 2001). The use of high temperature or pressure partially or completely unfolded protein and granted water accessibility to tryptophan. Indeed, the Raman spectra provided another evidence of this temperature/pressure denaturation of protein by the shifting and broadening of the amide I band as discussed above. Unlike heating, steaming and high pressure, although fluorescence of Endo3-, Tail21- and NaCl meat increased compared to raw meat, there was no red shift of emission wavelength. Therefore, the interpretation for the intensity increase might be related to the modification of surface hydrophobicity of protein caused by ionic effect from salt. It is noteworthy that Endo3 and Tail21 solution each contained 2% NaCl, equal to concentration of NaCl sample. Jiang et al. (2015) reported that ionic effects from salt loosened the protein structure and resulted in the modification of surface amino acid distribution, i.e. more fluorescent amino acid residues exposed on the surface of protein.

Peaks at 330/390 nm, 330/410 nm and 330/490 nm excitation/emission wavelengths were assigned to collagen type V (the first peak) and collagen type I (the latter two peaks) (Andersen & Wold, 2003). Both collagen type I and V were abundantly found in shrimp shell, whereas only collagen type I was found in shrimp meat. Collagen from shrimp shell was similar to collagen from salmon with respect to autofluorescence characteristics studied by Andersen and Wold (2003). Fujimoto, Akiba, and Nakamura (1977) reported that collagen crosslinks, e.g. pyridinoline, was responsible for collagen fluorescence.

Collagen fluorescence was more intense in all treated shells than in raw shell. When interpreting predominance of collagen, some authors linked it to energy transfer or absorbance of other compounds. In the angle of energy transfer, pressure resulted in hindrance of energy transfer from red pigments (predominantly astaxanthin) to collagen molecule (Foguel, Chaloub, Silva, Crofts, & Weber, 1992). In the angle of absorbance of other compounds, Andersen and Wold (2003) discussed that because these red pigments absorbed light strongly in the region 350 – 520 nm, re-absorbance of collagen fluorescence

might occur, thus fluorescence intensity of collagen was weaker in pigmented materials than non-pigmented materials. In both explanations, pigments were associated with the intensity of collagen fluorescence. In contrast, in the present study, the pigments were not found to affect the collagen fluorescence. For instance, high pressure increased the fluorescence intensity of shell (fluorescence examined), but the pigments were almost unchanged (Raman examined). Therefore, the increased fluorescence of high-pressure-induced shell may not relate to the pigments. In this context, conformational changes of collagen structure might be the cause of changes in its fluorescence intensity.

Shells treated with proteolytic enzymes (Endo3 and Tail21) both had collagen intensity increased as compared to raw shell. This increase was in good agreement with previous studies (Deyl, Sulcova, Praus, & Goldman, 1970; Fujimori, 1989), where enzymatic liberation of fluorescent amino acids or crosslinks was attributed to the phenomenon.

3.3.4. Mechanism of shell tightening

For high pressure, secondary structure of collagen in HP-treated shells, irrespective of pressure level, was not modified, which was evidenced by the unchanged amide I peak as compared to raw shell in Raman spectra. While the secondary structure was intact, the triple-helix structure of collagen was stabilized by high pressure (100 – 600 MPa), evidenced by increased helix-coil transition enthalpy. This stabilization could be explained by HP-shortened intramolecular and intermolecular hydrogen bonds and strengthened natural intermolecular crosslinks (HP100) or formation of new crosslinks (HP600). The new crosslinks or stabilized crosslinks emitted much stronger fluorescence in HP shells compared to raw shell. The difficulty in peeling shrimp at high pressure level therefore could be explained by interactions or crosslinks either strengthen the existing bonds or form new bonds, in both cases, could interact or link with materials in epidermis or meat, and consequently peelability was low (**Figure 5**).

For ohmic heating, secondary structure of collagen in OH50-treated shell was modified in which some α-helices are lost, evidenced by the blue shift of amide I peak, meaning that partial denaturation took place. The partial denaturation was also confirmed by DSC curve, in which transition temperature and enthalpy of collagen decreased as compared to raw shell. In excess water medium, partial denaturation of collagen also means partial gelatinization of collagen to gelatin. This gelatinization could contribute to the difficulty of peeling for shrimp preheated at high temperature (**Figure 5**). Although collagen structure has been unfolded to some extent, the fluorescence intensity of collagen was still stronger than raw shell. This suggests that the fluorescence intensity was sensitive to partial denaturation. A possible explanation for strong fluorescence of OH shell was that the partial denaturation exposed some hydrophobic bonds and crosslinks in the core of collagen to the surface, facilitating access to laser light.

4. Conclusion

Effects of high pressure and ohmic heating on peelability, thermal and structural properties of shrimp parts (shell and meat) were studied. For high pressure, mild HP conditions (pressure <350 MP, holding time ≤3 min) reduced the peeling work compared to raw shrimp, but increasing pressure and time led to an increase in the peeling work. Based on a RSM prediction model, an optimum condition of best peeling was obtained, i.e. 100 MPa for 3 min at 5°C, under which a peeling work of 6.6 mJ/g was needed to peel the shrimp. DSC thermogram and spectroscopic spectra showed that pressurizations at both 100 and 600 MPa minorly denatured myofibrillar proteins (myosin and actin) in meat, and HP600 obviously stabilized connective proteins (collagen) in epidermis and shell. The pressure-induced stabilization of collagen structure could be resulted from shortening existing hydrogen bonds and forming new hydrogen bonds in the triple-helix structure and/or stabilizing intermolecular crosslinks between collagen molecules. This resulted in a high peeling work of shrimp treated with high pressure level.

462 Ohmic heating as a blanching method did not improve the peelability of shrimp, and at some extreme
463 conditions (high temperature, voltage, salt concentration) the peeling work was much higher than the
464 control. Collagen gelatinization was responsible for this difficult peeling. When shrimp was ohmic heated
465 at a temperature higher than the shell collagen transition temperature (45°C), the triple-helix structure of
466 collagen molecule started to unfold into random coils that were able to reassemble into a gel matrix at
467 cooling condition. The gel glued the muscle-shell connection even stronger than the native connection.
468 Ohmic heating also denatured proteins in shrimp meat and caused loss of astaxanthin.

469 **Acknowledgements**

470 The authors are grateful to the Green Development and Demonstration Program (GUDP Denmark),
471 The Danish Agrifish Agency, the Ministry of Food, Agriculture and Fisheries for the financial support
472 to the project “Sustainable technologies for the optimization of shrimp production - TECHSHELL”
473 (Grant number 4009-14-0870, 2015).

474 **Conflict of interest**

475 Declarations of interest: none.

476 **References**

477 Alimova, A., Chakraverty, R., Muthukattil, R., Elder, S., Katz, A., Sriramoju, V., Lipper, S., & Alfano,
478 R. R. (2009). In Vivo Molecular Evaluation of Guinea Pig Skin Incisions Healing after Surgical
479 Suture and Laser Tissue Welding Using Raman Spectroscopy. *Journal of photochemistry and*
480 *photobiology. B, Biology, 96*(3), 178-183.

481 Allali, H., Marchal, L., & Vorobiev, E. (2010). Blanching of Strawberries by Ohmic Heating: Effects on
482 the Kinetics of Mass Transfer During Osmotic Dehydration. *Food and Bioprocess Technology,*
483 *3*(3), 406-414.

484 Andersen, C. M., & Wold, J. P. (2003). Fluorescence of Muscle and Connective Tissue from Cod and
485 Salmon. *Journal of Agricultural and Food Chemistry, 51*(2), 470-476.

486 Angsupanich, K., Edde, M., & Ledward, D. A. (1999). Effects of High Pressure on the Myofibrillar
487 Proteins of Cod and Turkey Muscle. *Journal of Agricultural and Food Chemistry, 47*(1), 92-99.

488 Angsupanich, K., & Ledward, D. A. (1998). High Pressure Treatment Effects on Cod (Gadus Morhua)
489 Muscle. *Food Chemistry, 63*(1), 39-50.

490 Bindu, J., Grinson, J., Kamalakanth, C. K., & Gopal, T. K. S. (2015). High Pressure Treatment of Green
491 Mussel Perna Viridis Linnaeus, 1758: Effect on Shucking and Quality Changes in Meat During
492 Chill Storage. *Indian Journal of Fisheries, 62*(2), 70-76.

493 Chen, L. Q., Ma, L., Zhou, M. R., Liu, Y., & Zhang, Y. H. (2014). Effects of Pressure on Gelatinization
494 of Collagen and Properties of Extracted Gelatins. *Food Hydrocolloids, 36*, 316-322.

495 Chen, X., Yang, H., Zhong, Z., & Yan, N. (2017). Base-Catalysed, One-Step Mechanochemical
496 Conversion of Chitin and Shrimp Shells into Low Molecular Weight Chitosan. *Green Chemistry,*
497 *19*(12), 2783-2792.

Dang, T. T., Gringer, N., Jessen, F., Olsen, K., Bøknæs, N., Nielsen, P. L., & Orlien, V. (2018a). Emerging and Potential Technologies for Facilitating Shrimp Peeling: A Review. *Innovative Food Science & Emerging Technologies, 45*, 228-240.

Dang, T. T., Gringer, N., Jessen, F., Olsen, K., Bøknæs, N., Nielsen, P. L., & Orlien, V. (2018b). Enzyme-Assisted Peeling of Cold Water Shrimps (Pandalus Borealis). *Innovative Food Science & Emerging Technologies, 47*, 127-135.

Dang, T. T., Gringer, N., Jessen, F., Olsen, K., Bøknæs, N., Nielsen, P. L., & Orlien, V. (2018c). Facilitating Shrimp (Pandalus Borealis) Peeling by Power Ultrasound and Proteolytic Enzyme. *Innovative Food Science & Emerging Technologies, 47*, 525-534.

David, C., Foley, S., Mavon, C., & Enescu, M. (2008). Reductive Unfolding of Serum Albumins Uncovered by Raman Spectroscopy. *Biopolymers, 89*(7), 623-634.

Deyl, Z., Sulcova, H., Praus, R., & Goldman, J. N. (1970). A Fluorescent Compound in Collagen and Its Relation to Age of Animal. *Experimental Gerontology, 5*(1), 57-&.

Dufour, É., Frencia, J. P., & Kane, E. (2003). Development of a Rapid Method Based on Front-Face Fluorescence Spectroscopy for the Monitoring of Fish Freshness. *Food Research International, 36*(5), 415-423.

Egelandsdal, B., Wold, J. P., Sponnich, A., Neegård, S., & Hildrum, K. I. (2002). On Attempts to Measure the Tenderness of Longissimus Dorsi Muscles Using Fluorescence Emission Spectra. *Meat Science, 60*(2), 187-202.

ElMasry, G., Nagai, H., Moria, K., Nakazawa, N., Tsuta, M., Sugiyama, J., Okazaki, E., & Nakauchi, S. (2015). Freshness Estimation of Intact Frozen Fish Using Fluorescence Spectroscopy and Chemometrics of Excitation–Emission Matrix. *Talanta, 143*, 145-156.

ElMasry, G., Nakazawa, N., Okazaki, E., & Nakauchi, S. (2016). Non-Invasive Sensing of Freshness Indices of Frozen Fish and Fillets Using Pretreated Excitation–Emission Matrices. *Sensors and Actuators B: Chemical, 228*, 237-250.

Foguel, D., Chaloub, R. M., Silva, J. L., Crofts, A. R., & Weber, G. (1992). Pressure and Low Temperature Effects on the Fluorescence Emission Spectra and Lifetimes of the Photosynthetic Components of Cyanobacteria. *Biophysical Journal, 63*(6), 1613-1622.

Fujimori, E. (1989). Cross-Linking and Fluorescence Changes of Collagen by Glycation and Oxidation. *Biochimica Et Biophysica Acta, 998*(2), 105-110.

Fujimoto, D., Akiba, K. Y., & Nakamura, N. (1977). Isolation and Characterization of A Fluorescent Material in Bovine Achilles-Tendon Collagen. *Biochemical and Biophysical Research Communications, 76*(4), 1124-1129.

Gringer, N., Dang, T. T., Orlien, V., Olsen, K., Boknaes, N., & Jessen, F. (2018). A Quantitative Method to Measure and Evaluate the Peelability of Shrimps (Pandalus Borealis). *Lwt-Food Science and Technology, 94*, 20-24.

Hassoun, A., & Karoui, R. (2017). Quality Evaluation of Fish and Other Seafood by Traditional and Nondestructive Instrumental Methods: Advantages and Limitations. *Critical Reviews in Food Science and Nutrition, 57*(9), 1976-1998.

He, H., Adams, R. M., Farkas, D. F., & Morrissey, M. T. (2002). Use of High-Pressure Processing for Oyster Shucking and Shelf-Life Extension. *Journal of Food Science, 67*(2), 640-645.

Hejazi, M., Behzad, T., Heidarian, P., & Nasri-Nasrabadi, B. (2018). A Study of the Effects of Acid, Plasticizer, Cross-Linker, and Extracted Chitin Nanofibers on the Properties of Chitosan Biofilm. *Composites Part a-Applied Science and Manufacturing, 109*, 221-231.

Herrero, A. M. (2008). Raman Spectroscopy for Monitoring Protein Structure in Muscle Food Systems. *Critical Reviews in Food Science and Nutrition, 48*(6), 512-523.

544 Heu, M. S., Kim, J. S., & Shahidi, F. (2003). Components and Nutritional Quality of Shrimp Processing
545 by-Products. *Food Chemistry, 82*(2), 235-242.
546 Hsu, K. C., Hwang, J. S., Chi, H. Y., & Lai, K. M. (2010). Effect of Different High Pressure Treatments
547 on Shucking, Biochemical, Physical and Sensory Characteristics of Oysters to Elaborate a
548 Traditional Taiwanese Oyster Omelette. *Journal of the Science of Food and Agriculture, 90*(3),
549 530-535.
550 Jaeger, H., Roth, A., Toepfl, S., Holzhauser, T., Engel, K. H., Knorr, D., Vogel, R. F., Bandick, N.,
551 Kulling, S., Heinz, V., & Steinberg, P. (2016). Opinion on the Use of Ohmic Heating for the
552 Treatment of Foods. *Trends in Food Science & Technology, 55*, 84-97.
553 Jiang, L., Wang, Z., Li, Y., Meng, X., Sui, X., Qi, B., & Zhou, L. (2015). Relationship between Surface
554 Hydrophobicity and Structure of Soy Protein Isolate Subjected to Different Ionic Strength.
555 *International Journal of Food Properties, 18*(5), 1059-1074.
556 Karoui, R., & Blecker, C. (2011). Fluorescence Spectroscopy Measurement for Quality Assessment of
557 Food Systems - A Review. *Food and Bioprocess Technology, 4*(3), 364-386.
558 Kopp, J., Bonnet, M., & Renou, J. P. (1990). Effect of Collagen Crosslinking on Collagen-Water
559 Interactions (A Dsc Investigation). *Matrix, 9*(6), 443-450.
560 Lascorz, D., Torella, E., Lyng, J. G., & Arroyo, C. (2016). The Potential of Ohmic Heating as an
561 Alternative to Steam for Heat Processing Shrimps. *Innovative Food Science & Emerging*
562 *Technologies, 37*, 329-335.
563 LiChan, E. C. Y. (1996). The Applications of Raman Spectroscopy in Food Science. *Trends in Food*
564 *Science & Technology, 7*(11), 361-370.
565 Mesias, M., Wagner, M., George, S., & Morales, F. J. (2016). Impact of Conventional Sterilization and
566 Ohmic Heating on the Amino Acid Profile in Vegetable Baby Foods. *Innovative Food Science &*
567 *Emerging Technologies, 34*, 24-28.

568 Nan, J., Zou, M. L., Wang, H. B., Xu, C. Z., Zhang, J. T., Wei, B. M., He, L., & Xu, Y. L. (2018). Effect
569 of Ultra-High Pressure on Molecular Structure and Properties of Bullfrog Skin Collagen.
570 *International Journal of Biological Macromolecules, 111*, 200-207.
571 Ngarize, S., Herman, H., Adams, A., & Howell, N. (2004). Comparison of Changes in the Secondary
572 Structure of Unheated, Heated, and High-Pressure-Treated Ss-Lactoglobulin and Ovalbumin
573 Proteins Using Fourier Transform Raman Spectroscopy and Self-Deconvolution. *Journal of*
574 *Agricultural and Food Chemistry, 52*(21), 6470-6477.
575 Nonaka, M., Lichan, E., & Nakai, S. (1993). Raman-Spectroscopic Study of Thermally-Induced Gelation
576 of Whey Proteins. *Journal of Agricultural and Food Chemistry, 41*(8), 1176-1181.
577 Ong, L. K., Danujatmiko, Z., Aylianawati, & Sudaryanto, Y. (2014). *The Prospect of Shrimp Shell Waste*
578 *as Raw Material in the Gelatin Production* (Vol. 9).
579 Pedersen, S. J., Feyissa, A. H., Kavli, S. T. B., & Frosch, S. (2016). An Investigation on the Application
580 of Ohmic Heating of Cold Water Shrimp and Brine Mixtures. *Journal of Food Engineering, 179*,
581 28-35.
582 Potekhin, S. A., Senin, A. A., Abdurakhmanov, N. N., & Tiktopulo, E. I. (2009). High Pressure
583 Stabilization of Collagen Structure. *Biochimica Et Biophysica Acta-Proteins and Proteomics,*
584 *1794*(8), 1151-1158.
585 Rahman, M. A., & Halfar, J. (2014). First Evidence of Chitin in Calcified Coralline Algae: New Insights
586 into the Calcification Process of Clathromorphum Compactum. *Scientific Reports, 4*, 6162.
587 Rau, J. V., Fosca, M., Graziani, V., Taffon, C., Rocchia, M., Caricato, M., Pozzilli, P., Muda, A. O., &
588 Crescenzi, A. (2017). Proof-of-Concept Raman Spectroscopy Study Aimed to Differentiate
589 Thyroid Follicular Patterned Lesions. *Scientific Reports, 7*.

590 Rodde, R. H., Einbu, A., & Varum, K. M. (2008). A Seasonal Study of the Chemical Composition and
591 Chitin Quality of Shrimp Shells Obtained from Northern Shrimp (Pandalus Borealis).
592 *Carbohydrate Polymers, 71*(3), 388-393.
593 Rødde, R. H., Einbu, A., & Vårum, K. M. (2008). A Seasonal Study of the Chemical Composition and
594 Chitin Quality of Shrimp Shells Obtained from Northern Shrimp (*Pandalus Borealis*).
595 *Carbohydrate Polymers, 71*(3), 388-393.
596 Raabe, D., Romano, P., Sachs, C., Fabritius, H., Al-Sawalmih, A., Yi, S., Servos, G., & Hartwig, H. G.
597 (2006). Microstructure and Crystallographic Texture of the Chitin-Protein Network in the
598 Biological Composite Material of the Exoskeleton of the Lobster Homarus Americanus.
599 *Materials Science and Engineering a-Structural Materials Properties Microstructure and*
600 *Processing, 421*(1-2), 143-153.
601 Schubring, R. (2005). Characterizing Protein Changes Caused by Application of High Hydrostatic
602 Pressure on Muscle Food by Means of Dsc. *Journal of Thermal Analysis and Calorimetry, 82*(1),
603 229-237.
604 Schubring, R. (2009). Comparative Study of Dsc Pattern, Colour and Texture of Shrimps During Heating.
605 *Journal of Thermal Analysis and Calorimetry, 95*(3), 749.
606 Sengun, I. Y., Turp, G. Y., Icier, F., Kendirci, P., & Kor, G. (2014). Effects of Ohmic Heating for Pre-
607 Cooking of Meatballs on Some Quality and Safety Attributes. *Lwt-Food Science and Technology,*
608 *55*(1), 232-239.
609 Sriket, P., Benjakul, S., Visessanguan, W., & Kijroongrojana, K. (2007). Comparative Studies on
610 Chemical Composition and Thermal Properties of Black Tiger Shrimp (*Penaeus Monodon*) and
611 White Shrimp (*Penaeus Vannamei*) Meats. *Food Chemistry, 103*(4), 1199-1207.
612 Swatland, H. J., Nielsen, T., & Andersen, J. R. (1995). Correlations of Mature Beef Palatability with
613 Optical Probing of Raw Meat. *Food Research International, 28*(4), 403-416.

614 Verhaeghe, T., Vlaemynck, G., De Block, J., Van Weyenberg, S., Braeckman, R., & Hendrickx, M.
615 (2016). Kinetics of Heat Induced Muscle Protein Denaturation of Brown Shrimp (Crangon
616 Crangon). *Journal of Food Engineering, 191*, 88-94.
617 Vivian, J. T., & Callis, P. R. (2001). Mechanisms of Tryptophan Fluorescence Shifts in Proteins.
618 *Biophysical Journal, 80*(5), 2093-2109.
619 Voisin, E. A. (2001). *U.S Patent No. 6,217,435 B1*. Washington, DC: U.S. Patent and Trademark Office.
620 Wasswa, J., Tang, R., & Gu, X. H. (2007). Utilization of Fish Processing by-Products in the Gelatin
621 Industry. *Food Reviews International, 23*(2), 159-174.
622 Wongsa-Ngasri, P., & Sastry, S. K. (2015). Effect of Ohmic Heating on Tomato Peeling. *Lwt-Food*
623 *Science and Technology, 61*(2), 269-274.
624 Wongsa-Ngasri, P., & Sastry, S. K. (2016a). Tomato Peeling by Ohmic Heating with Lye-Salt
625 Combinations: Effects of Operational Parameters on Peeling Time and Skin Diffusivity. *Journal*
626 *of Food Engineering, 186*, 10-16.
627 Wongsa-Ngasri, P., & Sastry, S. K. (2016b). Tomato Peeling by Ohmic Heating: Effects of Lye-Salt
628 Combinations and Post-Treatments on Weight Loss, Peeling Quality and Firmness. *Innovative*
629 *Food Science & Emerging Technologies, 34*, 148-153.
630 Yang, H., Li, J., Yu, Y., Zheng, W., Zhu, S., & Hu, Y. (2010). *High Pressure Shelling of Shrimp and*
631 *Quality Improvement.* Paper presented at the American Society of Agricultural and Biological
632 Engineers Annual International Meeting 2010, ASABE 2010.
633 Zell, M., Lyng, J. G., Cronin, D. A., & Morgan, D. J. (2010). Ohmic Cooking of Whole Turkey Meat -
634 Effect of Rapid Ohmic Heating on Selected Product Parameters. *Food Chemistry, 120*(3), 724-
635 729.
636

637 **Table 1.** Effect of ohmic heating on shrimp peelability

Salt (%)	Voltage (V)	Temperature (°C)	Peeling Work (mJ/g)	Three-way ANOVA	
				Effect term	*p* value
0	0	0	4.2 ± 2.1^{de}	Salt	<0.0001
2	92	30	4.7 ± 1.9^{de}	Voltage	<0.0001
2	92	35	4.0 ± 1.9^{de}	Temperature	<0.0001
2	92	40	4.4 ± 1.4^{de}	Salt*Voltage	0.0096
2	92	50	5.5 ± 2.0^{bcde}	Salt*Temperature	0.0005
2	138	30	4.0 ± 1.2^{de}	Voltage*Temperature	0.1649
2	138	35	5.4 ± 3.0^{bcde}	Salt*Voltage*Temperature	0.1857
2	138	40	4.3 ± 1.5^{de}	Model	<0.0001
2	138	50	6.2 ± 2.0^{bcd}		
2	138	60	6.1 ± 2.0^{bcd}		
2	184	30	5.2 ± 2.5^{bcde}		
2	184	35	5.0 ± 2.4^{cde}		
2	184	40	4.3 ± 1.2^{de}		
2	184	50	5.7 ± 1.8^{bcde}		
2	184	60	5.5 ± 1.4^{bcde}		
10	92	30	3.5 ± 1.2^{e}		
10	92	35	5.5 ± 1.4^{bcde}		
10	92	40	5.4 ± 2.0^{bcde}		
10	92	50	6.2 ± 2.1^{bcd}		
10	138	20	4.4 ± 1.8^{de}		
10	138	30	5.6 ± 2.3^{bcde}		
10	138	35	6.2 ± 2.3^{bcd}		
10	138	40	7.2 ± 2.5^{bc}		
10	138	50	9.8 ± 1.9^{a}		
10	138	60	9.9 ± 2.5^{a}		
10	184	20	4.6 ± 1.7^{de}		
10	184	30	5.6 ± 2.0^{bcde}		
10	184	35	5.8 ± 2.6^{bcde}		
10	184	40	6.1 ± 2.1^{bcd}		
10	184	50	7.5 ± 3.1^{b}		

638 Values in the same column with different letters are significantly different at $p < 0.05$, based on Student-

639 Newman-Keuls test.

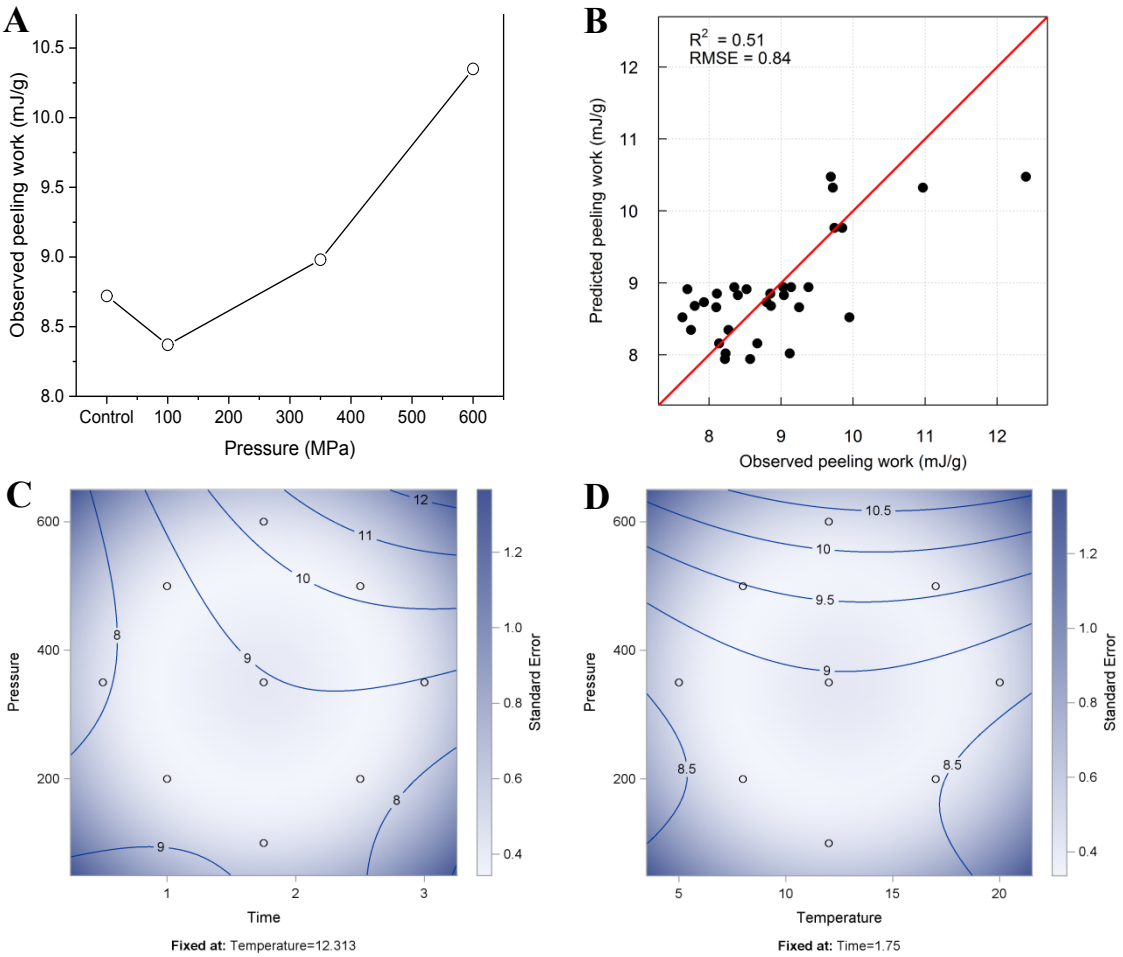

Figure 1. High pressure effect on shrimp peelability. (A) individual effect of pressure level on peeling work when fixing time at 1.75 min and temperature at 12.5°C, (B) observed vs. predicted values for peeling work obtained by response surface method, (C-D) contour plots of paired interaction of HP conditions on peeling work.

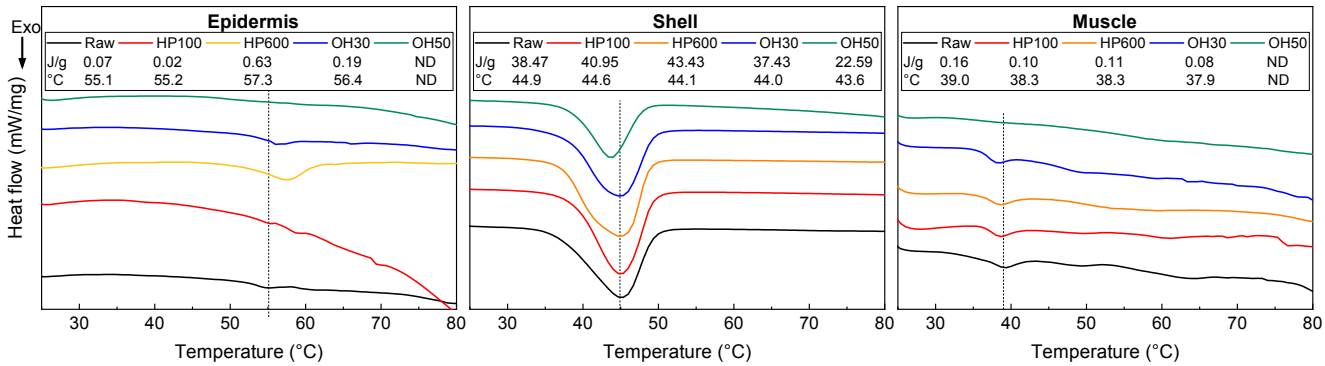

644 **Figure 2.** DSC thermogram of parts of shrimp under different conditions of high pressure and ohmic
645 heating processing. Raw, control shrimp; HP100, high pressure at 100 MPa; HP600, high pressure at 600
646 MPa; OH30, ohmic heating at 30°C; and OH50, ohmic heating at 50°C. Vertical dash line marks the
647 transition temperature of raw shrimp. ND = not detected, J/g = unit of enthalpy change (ΔH), °C = unit
648 of transition temperature of the peak marked with the dash line.

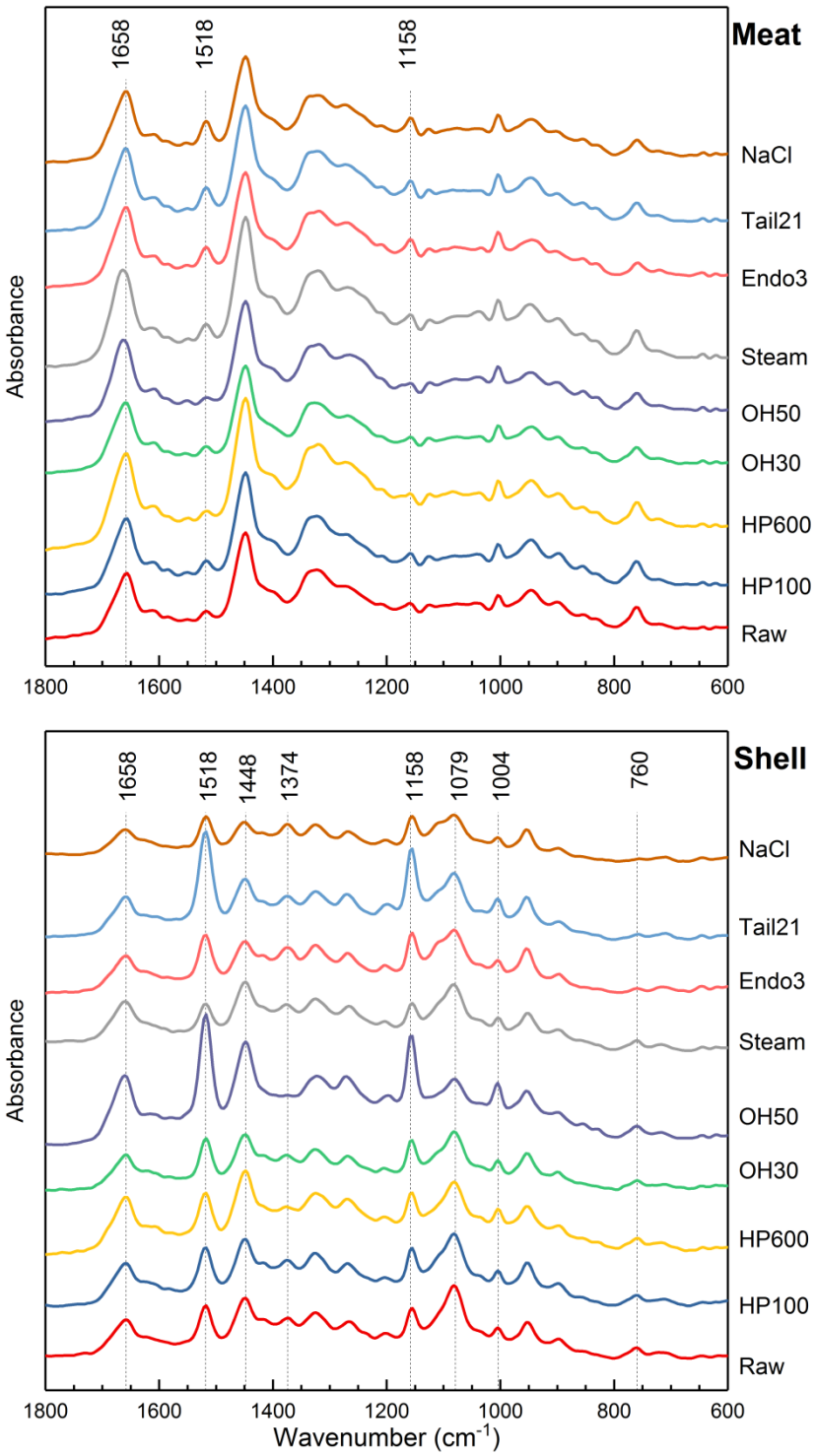

649 **Figure 3.** Raman spectra of meat and shell subjected to different treatments. Each spectrum is an average
650 of three spectra from three shrimp. Peaks with an arrow and numeric label are peaks modified by one of
651 the treatments in terms of intensity and visibility.

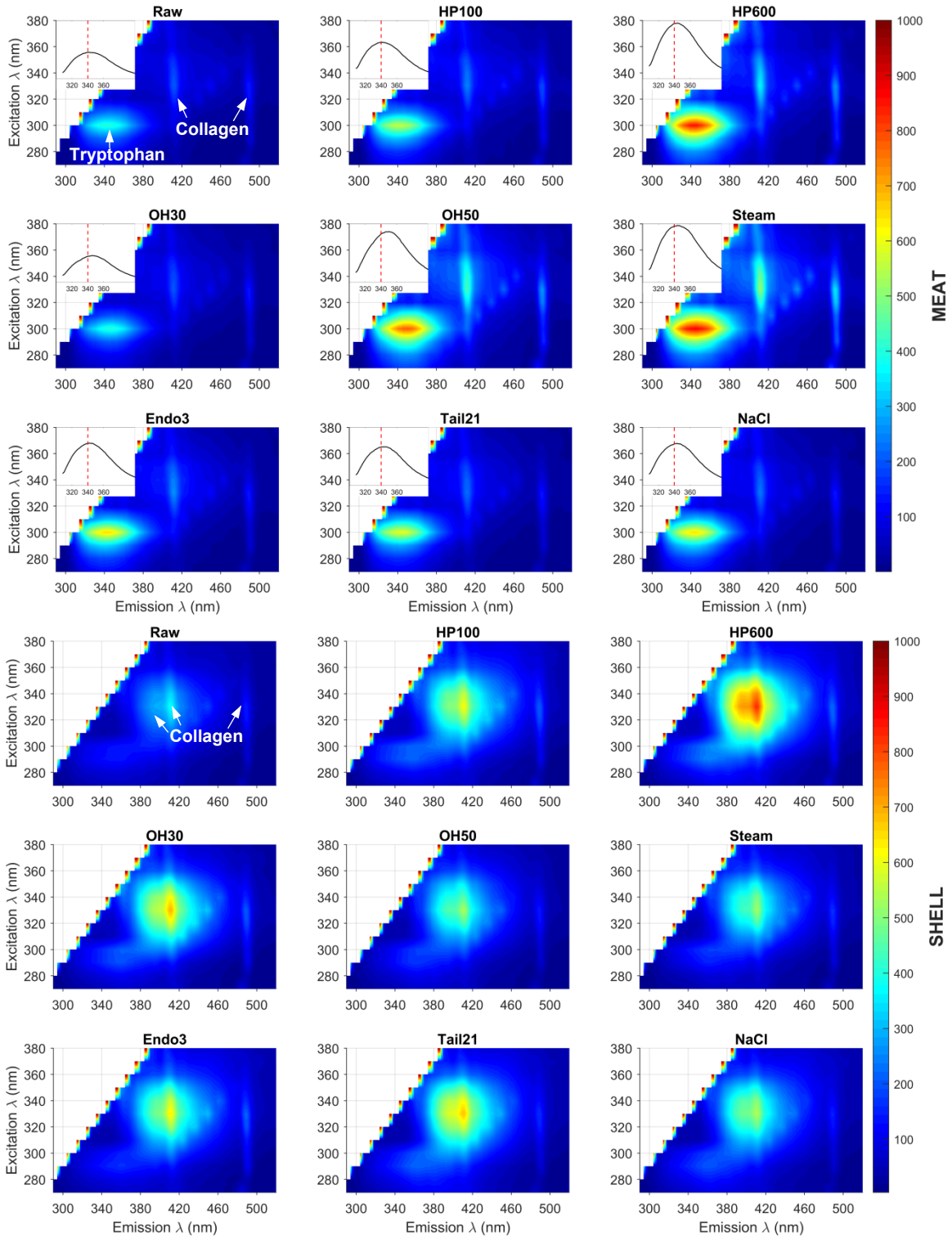

652

653 **Figure 4.** Fluorescence landscapes of shrimp meat and shell subjected to different treatments. Inset
654 figures in meat set represent emission fluorescence spectra of tryptophan at 300-nm excitation, and the
655 red dash line positions at 340-nm emission. Color bars on the right indicates the fluorescence intensity.

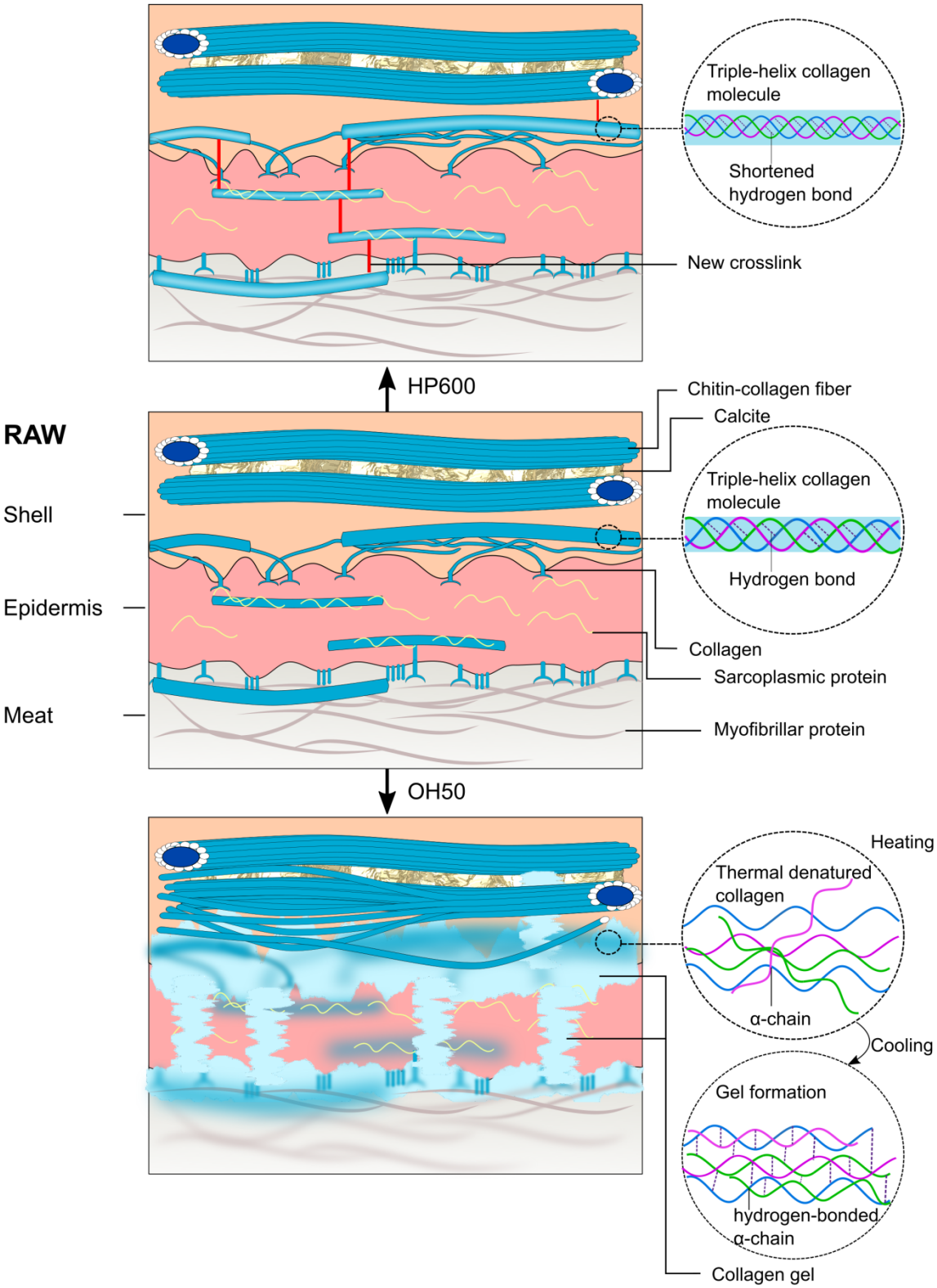

656 **Figure 5.** Proposed mechanism of shell tightening of shrimp caused by extreme conditions of high
657 pressure (600 MPa) and ohmic heating (50°C).